Open Quantum System Dynamics from Infinite Tensor Network Contraction

Valentin Link, Hong-Hao Tu, and Walter T. Strunz
Institut für Theoretische Physik, Technische Universität Dresden, D-01062, Dresden, Germany

(Received 10 November 2023; accepted 9 April 2024; published 16 May 2024)

Approaching the long-time dynamics of non-Markovian open quantum systems presents a challenging task if the bath is strongly coupled. Recent proposals address this problem through a representation of the so-called process tensor in terms of a tensor network. We show that for Gaussian environments highly efficient contraction to a matrix product operator (MPO) form can be achieved with infinite MPO evolution methods, leading to significant computational speed-up over existing proposals. The result structurally resembles open system evolution with carefully designed auxiliary degrees of freedom, as in hierarchical or pseudomode methods. Here, however, these degrees of freedom are generated automatically by the MPO evolution algorithm. Moreover, the semigroup form of the resulting propagator enables us to explore steady-state physics, such as phase transitions.

DOI: 10.1103/PhysRevLett.132.200403

Introduction.—Dissipative effects are crucial to our understanding of real world quantum mechanical systems and feature a variety of relevant physical phenomena absent in purely unitary settings. In many realistic and particularly interesting setups, the timescales of system and environment do not separate, leading to a buildup of strong correlations with the environment [1–7]. Then, advanced numerical tools are required for the simulation of the dynamics on a classical computer [8–13].

Many of the most sophisticated approaches realize the open system evolution by substituting the original environment with few physical or nonphysical auxiliary degrees of freedom. These auxiliary degrees of freedom must be carefully tailored to accurately reproduce the dynamics of the original bath. Prominent methods in this category include the well-established HEOM (hierarchical equations of motion) [8], HOPS (hierarchy of pure states) [14,15], and pseudomode approaches [16–18], among others [19–21]. However, identifying suitable auxiliary environments is generally a complex task that depends nontrivially on the specific characteristics of the bath structure [22–24]. A different strategy to treat open system dynamics avoids this issue by working directly with the exact influence functional [25]. Viewed as a process tensor, it encapsulates all dynamical properties of the reduced dynamics [26]. This tensor has a representation as a two-dimensional tensor network [11,27–29], which can be contracted to matrix product operator (MPO) form to allow for efficient computations [28–33]. MPO methods are also used widely in the context of weakly dissipative open systems with spatial correlations (see, e.g., [34,35]). In contrast, here, the MPO encodes temporal correlations due to time-nonlocal dynamics induced by a structured bath.

In this Letter we establish an alternative representation of the process tensor in terms of an infinite tensor network. This key result allows us to use infinite time evolving block decimation (iTEBD) [36] for network contraction, leading to a fast algorithm with a previously unachieved numerical scaling (linear in the bath memory time). The resulting MPO representation of the process tensor has the same structure as for methods using auxiliary degrees of freedom, bridging a gap between the two different approaches. Crucially, this delivers a single time-local propagator, encoding the full dynamics of the open system. Thus, we can reach arbitrary evolution times straightforwardly, and even utilize spectral theory in order to determine stationary states and characterize asymptotic behavior. In contrast to established methods such as HEOM, the auxiliary degrees of freedom are generated automatically in an optimized and systematic way by the network contraction algorithm.

Open system evolution.—As a model for open system dynamics we consider the standard Hamiltonian

$$H(t) = H_{\mathrm{syst}}(t) \otimes \mathbb{1}_{\mathrm{env}} + S \otimes B(t), \tag{1}$$

where H_{syst} and S are Hermitian operators in the Hilbert space of the system and $B(t)$ is an operator that describes the collective degrees of freedom of a Gaussian environment consisting of a continuum of bosonic modes [1]. This operator is characterized by the so-called bath correlation function $\alpha(t,s) = \mathrm{tr}\rho_{\mathrm{env}}(0)B(t)B(s)$, where $\rho_{\mathrm{env}}(0)$ is a Gaussian environment initial state [37]. The bath is said to be stationary if the bath correlation function depends only on the time difference $\alpha(t,s) \equiv \alpha(t-s)$. While notable exceptions exist [38], this is the standard scenario in open system dynamics. In order to arrive at a description of the reduced dynamics in terms of the process tensor, one can employ a Trotter splitting of the full unitary time evolution operator in small time steps Δ [39]. Then, a time-discrete

path integral for the dynamics can be derived, in which the influence of the bath is fully captured by the so-called influence functional. In a more general modern open system framework, the influence functional gives rise to the process tensor from which all dynamical properties of the system can be extracted [26,28].

For clarity we focus only on computing the system density matrix after N time steps $t = N\Delta$. We use a Liouville-space (density matrix space) notation where a single index $\mu \equiv (\mu_l, \mu_r)$ labels a ("left" and "right") pair of eigenstates $|\mu_l\rangle$, $|\mu_r\rangle$ of the coupling operator S, such that density matrices are denoted as vectors $\rho^\mu = \langle \mu_l|\rho|\mu_r\rangle$. Thus, if the dimension of the system Hilbert space is d, μ runs from 1 to d^2. The time evolution of the system state $\rho(t)$ can then be expressed in terms of a discrete path integral [28,40–42]

$$\rho^{\nu_N}(N\Delta) = \sum_{\substack{\mu_1 \ldots \mu_N \\ \nu_0 \ldots \nu_{N-1}}} \mathcal{F}_N^{\mu_1 \ldots \mu_N} \left(\prod_{k=1}^{N} \mathcal{U}_k^{\nu_{k-1}\mu_k\nu_k} \right) \rho^{\nu_0}(0). \quad (2)$$

We can write this equation pictorially using tensor network notation

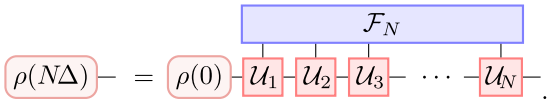

(3)

The tensors $\mathcal{U}_k^{\lambda\mu\nu}$ can be seen as unitary channels describing the evolution due to H_{syst} for the time step k [43] and $\mathcal{F}_N^{\mu_1 \ldots \mu_N}$ is the time-discrete influence functional, a rank-N tensor accounting for the time-nonlocal effect of the bath.

Even though for Gaussian baths the influence functional is known analytically, the time evolution according to Eq. (2) involves a sum over all elements of $\mathcal{F}_N$ which are exponentially many (d^{2N}). Therefore such a direct computation cannot be used in practice.

Tensor network representation of the influence functional.—It has been shown in Refs. [11,27,28] that the time-discrete influence functional can be represented as a two-dimensional tensor network. In detail one can define a set of elementary tensors

$$b_{ij}^{\mu\nu}(k) = \begin{cases} \delta_{ij}\delta_{\mu\nu} I_k(\mu, j), & k > 0 \\ \delta_{ij}\delta_{\mu\nu}\delta_{j\mu} I_0(\mu, j), & k = 0 \end{cases} \quad (4)$$

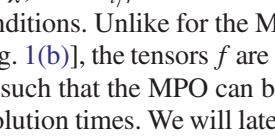

such that the influence functional can be expressed as in Fig. 1(a). Here the weights

$$I_k(\nu, \mu) = \exp\left(-(S_{\mu_l} - S_{\mu_r})(\eta_k S_{\nu_l} - \eta_k^* S_{\nu_r})\right) \quad (5)$$

are used, where η_k is determined by the bath correlation function at time step k and S_n denotes the nth eigenvalue of

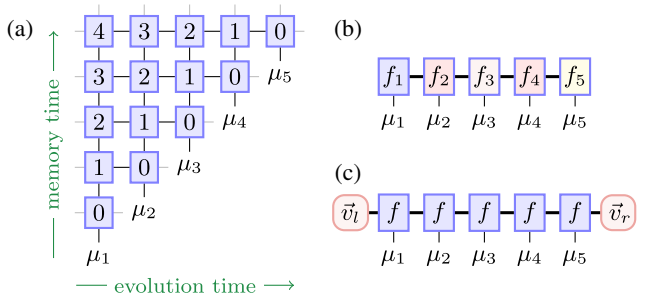

FIG. 1. Different tensor network representation of the time discrete influence functional $\mathcal{F}_5^{\mu_1 \cdots \mu_5}$ for $N = 5$ time steps. (a) Exact representation as a two-dimensional tensor network [28] (grayed out open tensor legs must be summed over). (b) Matrix product operator representation as obtained from contraction of the network (a) (PT-TEMPO) [30]. (c) A semigroup representation with identical tensors f, as in Eq. (6).

the coupling operator [11,28,43]. In the process tensor time evolving matrix product operators (PT-TEMPO) scheme [11,28,30,45], the network [Fig. 1(a)] is contracted to a matrix product operator [Fig. 1(b)]. This can be done, for instance, by multiplying adjacent columns followed by a compression based on singular value decompositons, which is required to keep the bond dimension manageable. With a MPO form for the influence functional the open system evolution Eqs. (2), (3) can be performed straightforwardly with iterative tensor contractions. At first sight, to obtain a process tensor for N time steps in MPO form, $\mathcal{O}(N^2)$ matrix factorizations are required to contract the two-dimensional network Fig. 1(a). However, usually one assumes a finite memory time of the bath such that all $b(k)$ tensors for $k > N_c$ can be neglected ($\eta_{k>N_c} \approx 0$) [46]. In this case it has been shown that the scaling of the network contraction can be improved to $\mathcal{O}(N_c \log N_c)$ [47].

In the following we utilize infinite MPO evolution techniques to generate a new MPO representation for the influence functional, taking the uniform structure displayed in Fig. 1(c). As a formula we can express this as

$$\mathcal{F}_N^{\mu_1 \cdots \mu_N} = \vec{v}_l^T f^{\mu_1} f^{\mu_2} \cdots f^{\mu_N} \vec{v}_r, \quad (6)$$

where, for given index μ, f^μ is a square matrix (dimensions $\chi \times \chi$) and $\vec{v}_{l/r}$ are vectors realizing finite-time boundary conditions. Unlike for the MPO resulting from PT-TEMPO [Fig. 1(b)], the tensors f are all identical and independent of N, such that the MPO can be trivially extended to arbitrary evolution times. We will later exploit the crucial advantages of this semigroup structure in example calculations. As an important side remark, note that, when using auxiliary degrees of freedom to effectively describe the open system evolution, the time-discrete influence functional also takes the form of Eq. (6). For instance, using the hierarchical equations of motion (HEOM) approach, the tensor f becomes the propagator of the hierarchy for a time step Δ and the bond dimension χ is the number of auxiliary

density operators [43]. However, in order to generate the HEOM propagator one has to manually tailor a suitable auxiliary environment. In contrast, our new scheme automatically generates this form in an optimized way based on MPO compression.

As a first step we expand the exact network Fig. 1(a) by extending the index dimension (d^2) of the tensors $b(k)$ by one, introducing a "zero" dimension via $I_k(0,i) = I_k(i,0) \equiv 1$, and keeping the definition (4) as is. This additional dimension is used only to realize finite-size boundary conditions [boundary vectors in (6)] and can be discarded later. If one index of an extended $b(k)$ tensor is zero, the tensor reduces to a trivial product of delta functions. As demonstrated in the Supplemental Material [43], this property allows us to obtain the influence functional for $M < N$ time steps from the influence functional for N time steps by inserting zeros at the boundary

$$\mathcal{F}_M^{\mu_1\ldots\mu_M} = \mathcal{F}_N^{0\ldots0,\mu_1\ldots\mu_M} = \mathcal{F}_N^{\mu_1\ldots\mu_M,0\ldots0}. \tag{7}$$

It is even possible to factor the influence functional into two, by piercing the train of indices with at least N_c zeros

$$\mathcal{F}_N^{\mu_1\ldots\mu_M,0\ldots0,\nu_1\ldots\nu_K} = \mathcal{F}_M^{\mu_1\ldots\mu_M}\mathcal{F}_K^{\nu_1\ldots\nu_K}. \tag{8}$$

These relations can be used to obtain $\mathcal{F}_N$ from an influence functional $\mathcal{F}_\infty$ with infinite time steps. In fact, infinite tensor network contraction methods allow us to obtain an MPO expression for such an infinite influence functional in the form

$$\mathcal{F}_\infty^{\ldots\mu\nu\delta\ldots} = \mathrm{tr}[\cdots f^\mu f^\nu f^\delta \cdots], \tag{9}$$

where f^μ are $\chi\times\chi$ matrices (bond dimension χ, $\mu = 0, 1, \ldots, d^2$). As the boundary condition for the infinite network is irrelevant, we have chosen periodic boundary conditions for convenience. Using (7) and (8), the desired influence functional for N steps can then be obtained via

$$\mathcal{F}_N^{\mu_1\ldots\mu_N} = \mathrm{tr}[(f^0)^\infty f^{\mu_1} f^{\mu_2}\cdots f^{\mu_N}]. \tag{10}$$

The infinite matrix power can be expressed as $(f^0)^\infty = \vec{v}_r \otimes \vec{v}_l$ with $\vec{v}_{l/r}$ the leading left and right eigenvectors of f^0 (eigenvalue one). We have indeed recovered a representation of the type (6). Crucially, one only needs to compute and store the single tensor f instead of $\mathcal{O}(N_c)$ such tensors as in the finite contraction schemes [47]. Moreover, as demonstrated in the Supplemental Material [43], the stationary state can also be determined efficiently by computing the leading eigenvector of the full short-time propagator $\mathcal{Q}^{(\nu,j)}_{(\lambda,i)} = \sum_\mu f^\mu_{ij}\mathcal{U}^{\lambda\mu\nu}$ [43].

Algorithm.—It remains to provide an algorithm for computing the tensor f in Eq. (9). Based on an infinite-N limit of the exact network in Fig. 1(a), we propose a network contraction in an "anti-diagonal" direction starting from $k = N_c$, as shown in Fig. 2, when the network displays a structure suitable for time evolving block decimation (TEBD). The "gates" $b(k)$ can formally be seen as nearest neighbor coupling alternating between left and right "sites." Thus, it is straightforward to apply infinite TEBD algorithms [36,48,49] with MPO evolution from top to bottom (Fig. 2 right panel). This requires only N_c matrix factorizations. Since the gates $b(k)$ become weakly entangling for large k, the bond dimension increases significantly only for the last few evolution steps, making this an excellent contraction scheme. The simple iTEBD algorithm from Ref. [48] already performs very well, resulting in similar bond dimension for a given accuracy as the contraction of the finite network, but with a computational speedup in orders of magnitude (for more details on this computational advantage see the Supplemental Material [43]).

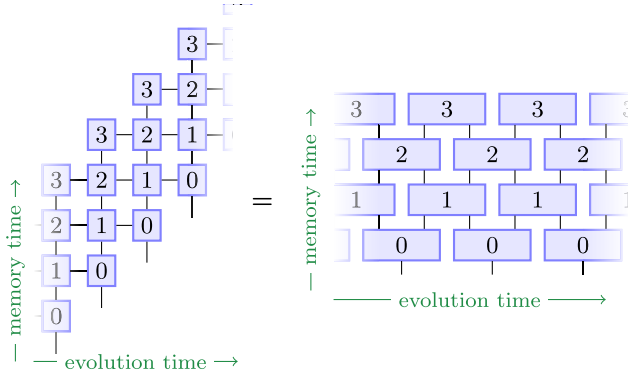

FIG. 2. Visual representation of an infinite time-translationally invariant influence functional with $N_c = 3$ (left network) which can be seen as nearest-neighbor matrix product operator evolution in memory time (right network).

Applications.—For the following examples we consider a (sub-)Ohmic bath with exponential cutoff. At zero temperature the bath correlation function reads [10]

$$\alpha(t) = \alpha\omega_c^2 \frac{\Gamma(s+1)}{2(1+\mathrm{i}\omega_c t)^{s+1}}. \tag{11}$$

In this expression, α is a dimensionless coupling strength, ω_c is the cutoff frequency, and $s \le 1$ is the exponent of the low frequency behavior $\propto \omega^s$ of the spectral density. This function decays algebraically for large times, possibly making it challenging for simulations due to a resulting long memory time.

As a first example we compute the asymptotic entanglement in a two-spin boson model. The model consists of noninteracting spins A and B that are coupled to the same bath via

$$H(t) = \frac{\Omega}{2}(\sigma_x^A + \sigma_x^B) \otimes \mathbb{1}_{\mathrm{env}} + \frac{1}{2}(\sigma_z^A + \sigma_z^B) \otimes B(t). \tag{12}$$

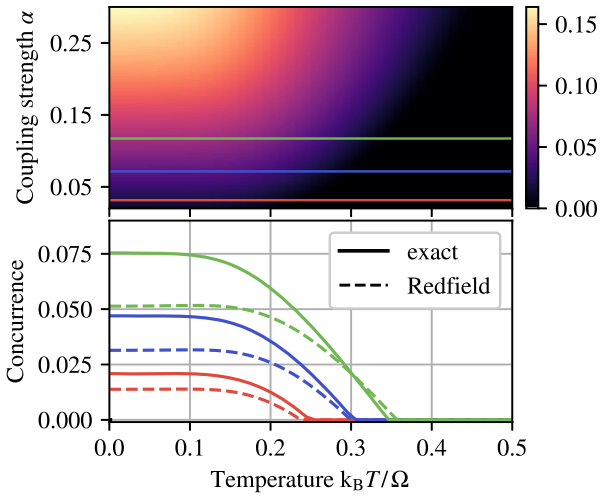

FIG. 3. Steady state concurrence in the two spin boson model with an Ohmic bath $s = 1$ and $\omega_c = 5\Omega$ for different coupling strengths and temperatures computed with our new approach (converged results). The lower panel shows cuts for the coupling strengths indicated by the lines in the upper panel. As a comparison, the concurrence predicted by Redfield theory is displayed as dashed lines.

Even if the spins are not directly coupled, at low temperatures, they still become entangled via the interaction with a common bath [2,50]. A crucial advantage of our framework is that we can use a spectral decomposition of $\mathcal{Q}$ to determine the steady state without relying on time evolution [51,52]. This allows us to effortlessly obtain accurate values for the asymptotic concurrence over large parameter regimes, displayed in Fig. 3. As can be expected, the concurrence increases with the increasing coupling strength and decreases with increasing temperature. For every coupling strength a maximum temperature exists after which the asymptotic state becomes separable. Note that even for weak coupling the concurrence is difficult to compute using standard perturbative master equations. As shown in Fig. 3, the second order Redfield equation [53] predicts systematically wrong values for weak coupling. In fact, second order master equations predict the steady state only to zeroth order accuracy [50,54,55], while obtaining higher order equations is tedious [55,56].

We further exemplify the power of a spectral analysis by studying the well-known quantum phase transition in the sub-Ohmic spin boson model [24,57–63]

$$H(t) = \Omega\sigma_x \otimes \mathbb{1}_{\mathrm{env}} + \sigma_z \otimes B(t). \tag{13}$$

As the coupling strength α is increased, the system changes from a symmetric phase, where asymptotically $\langle\sigma_z\rangle = 0$, to a symmetry broken phase $\langle\sigma_z\rangle \neq 0$. In general, such phase transitions are difficult to describe via time evolution because it is hard to separate asymptotic and transient behavior, especially since numerical approaches will typically generate a gapped spectrum [11,64]. In our framework we can employ a spectral decomposition in order to write the evolution of any observable as

$$\langle\sigma_z\rangle(t) = \sum_{k=1}^{\chi d^2} e^{\gamma_k t}\langle\sigma_z\rangle_k, \tag{14}$$

where γ_k are complex rates extracted from the eigenvalues of the short time propagator $\mathcal{Q}$. For large t we can keep only the two most relevant contributions in the sum, the leading and next-to-leading eigenvector

$$\langle\sigma_z\rangle(t) \to e^{\gamma_1 t}\langle\sigma_z\rangle_1 + e^{\gamma_2 t}\langle\sigma_z\rangle_2. \tag{15}$$

For the spin boson model this requires further justification, because the exact spectrum is not gapped. We provide a full discussion of the subtleties in the Supplemental Material [43]. There always exists a unique steady state contribution with $\gamma_1 = 0$ which obeys the symmetry of the model $\langle\sigma_z\rangle_1 = 0$. Hence, to describe the transition, we must consider the next-to-leading eigenvector. In order to ensure convergence of the algorithm, we modify the bath correlation function after a time t_r to decay exponentially (low frequency regularization). The original spin boson model is recovered when $t_r \to \infty$. In this limit we find for all coupling strengths that $\gamma_2 \to 0$ (see Fig. 4). Thus, the symmetry breaking is characterized by the value of $\langle\sigma_z\rangle_2$ extrapolated to large t_r. Since the phase transition is of second order, we make an extrapolation by fitting algebraic curves to the numerical data. The results are displayed

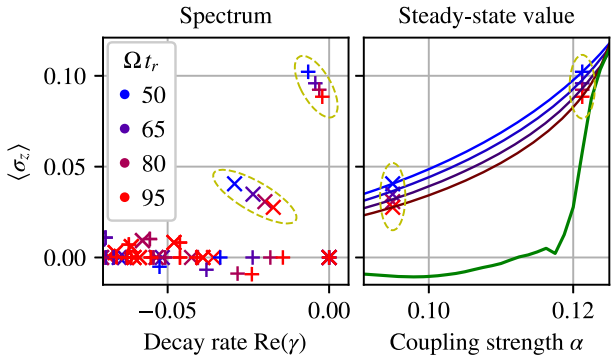

FIG. 4. Predictions for the stationary σ_z expectation value in the sub-Ohmic spin boson model ($s = 0.5$, $\omega_c = 20\Omega$) using different low frequency regularizations t_r. The left panel shows the spectral contributions to σ_z from the numerically computed short-time propagator below the transition (× marker) and above the transition (+ marker). We can identify the unique steady state ($\gamma = 0$, $\langle\sigma_z\rangle = 0$) as well as the next-to-leading contribution that breaks the symmetry (encircled). On the right-hand side the predicted steady state values are displayed as a function of the coupling strength. The green line shows the extrapolated values from algebraic fits [43]. We can identify the phase transition at $\alpha \approx 0.1175$.

in Fig. 4. While the curves for a finite t_r (red and blue) do not indicate the transition point, we can clearly identify the critical coupling from the extrapolated values (green curve).

Conclusions.—Matrix product operators have proven to be highly efficient in representing the temporal correlations (memory) in the quantum evolution of open systems [11,29,30,42]. These correlations are encoded in the influence functional (or the process tensor) which can be seen as a MPO in evolution time [28]. In this Letter we have demonstrated that, within this framework, a MPO form of the influence functional for arbitrary finite or infinite evolution times can be obtained by contraction of a single infinite tensor network. This strategy has crucial advantages over previous approaches that were based on finite tensor network contractions [28,47]. The new contraction algorithm achieves an optimal scaling with respect to the number of required matrix operations $\mathcal{O}(N_c)$ and leads to a considerable computational speed-up over all previously known approaches which require at least $\mathcal{O}(N_c \log N_c)$ (N_c is the number of memory time steps) [28,47]. Even more significantly, we obtain a single time-independent (semigroup) propagator that delivers the full open system evolution. This structural advantage allows us to utilize a spectral decomposition in order to characterize particularly relevant asymptotic dynamics even in difficult settings such as dissipative phase transitions. From a broader perspective, our result can be seen as a way to automatically generate an optimized set of auxiliary degrees of freedom which realize the exact bath response to a controlled level of accuracy. While the simple iTEBD algorithm that we use here performs very well already, we believe there is substantial potential for further optimization. For instance, using advanced infinite MPS evolution schemes [65–67] could lead to a better accuracy at a given bond dimension, which becomes relevant for large system sizes and ultrastrong coupling. Moreover, we are hopeful that similar schemes can be developed for more general couplings [33] as well as fermionic [68] and non-Gaussian baths [42].

V. L. and W. T. S. gratefully acknowledge discussions with Richard Hartmann concerning the numerical examples. We also thank Kai Müller, Jonathan Keeling, and anonymous referees for their valuable comments. H.-H. T. is supported by the Deutsche Forschungsgemeinschaft (DFG) through project A06 of SFB 1143 (Project No. 247310070).

[1] I. de Vega and D. Alonso, Dynamics of non-Markovian open quantum systems, Rev. Mod. Phys. **89**, 015001 (2017).
[2] M. Thorwart, J. Eckel, J. H. Reina, P. Nalbach, and S. Weiss, Enhanced quantum entanglement in the non-Markovian dynamics of biomolecular excitons, Chem. Phys. Lett. **478**, 234 (2009).
[3] P. Kaer, T. R. Nielsen, P. Lodahl, A.-P. Jauho, and J. Mørk, Non-Markovian model of photon-assisted dephasing by electron-phonon interactions in a coupled quantum-dot–cavity system, Phys. Rev. Lett. **104**, 157401 (2010).
[4] K. H. Madsen, S. Ates, T. Lund-Hansen, A. Löffler, S. Reitzenstein, A. Forchel, and P. Lodahl, Observation of non-Markovian dynamics of a single quantum dot in a micropillar cavity, Phys. Rev. Lett. **106**, 233601 (2011).
[5] S. Gröblacher, A. Trubarov, N. Prigge, G. D. Cole, M. Aspelmeyer, and J. Eisert, Observation of non-Markovian micromechanical Brownian motion, Nat. Commun. **6**, 7606 (2015).
[6] D. Segal and B. K. Agarwalla, Vibrational heat transport in molecular junctions, Annu. Rev. Phys. Chem. **67**, 185 (2016).
[7] A. Potočnik, A. Bargerbos, F. A. Y. N. Schröder, S. A. Khan, M. C. Collodo, S. Gasparinetti, Y. Salathé, C. Creatore, C. Eichler, H. E. Türeci, A. W. Chin, and A. Wallraff, Studying light-harvesting models with superconducting circuits, Nat. Commun. **9**, 2323 (2018).
[8] Y. Tanimura, Numerically, "exact" approach to open quantum dynamics: The hierarchical equations of motion (HEOM), J. Chem. Phys. **153**, 020901 (2020).
[9] H. Wang and M. Thoss, From coherent motion to localization: Dynamics of the spin-boson model at zero temperature, New J. Phys. **10**, 115005 (2008).
[10] R. Hartmann and W. T. Strunz, Exact open quantum system dynamics using the hierarchy of pure states (HOPS), J. Chem. Theory Comput. **13**, 5834 (2017).
[11] A. Strathearn, P. Kirton, D. Kilda, J. Keeling, and B. W. Lovett, Efficient non-Markovian quantum dynamics using time-evolving matrix product operators, Nat. Commun. **9**, 3322 (2018).
[12] M. Werther and F. Großmann, Apoptosis of moving nonorthogonal basis functions in many-particle quantum dynamics, Phys. Rev. B **101**, 174315 (2020).
[13] S. Kundu and N. Makri, PathSum: A C++ and Fortran suite of fully quantum mechanical real-time path integral methods for (multi-)system + bath dynamics, J. Chem. Phys. **158**, 224801 (2023).
[14] D. Suess, A. Eisfeld, and W. T. Strunz, Hierarchy of stochastic pure states for open quantum system dynamics, Phys. Rev. Lett. **113**, 150403 (2014).
[15] S. Flannigan, F. Damanet, and A. J. Daley, Many-body quantum state diffusion for non-Markovian dynamics in strongly interacting systems, Phys. Rev. Lett. **128**, 063601 (2022).
[16] A. Imamoglu, Stochastic wave-function approach to non-Markovian systems, Phys. Rev. A **50**, 3650 (1994).
[17] B. M. Garraway, Nonperturbative decay of an atomic system in a cavity, Phys. Rev. A **55**, 2290 (1997).
[18] F. Mascherpa, A. Smirne, A. D. Somoza, P. Fernández-Acebal, S. Donadi, D. Tamascelli, S. F. Huelga, and M. B. Plenio, Optimized auxiliary oscillators for the simulation of general open quantum systems, Phys. Rev. A **101**, 052108 (2020).
[19] K. H. Hughes, C. D. Christ, and I. Burghardt, Effective-mode representation of non-Markovian dynamics: A hierarchical approximation of the spectral density. I. Application to single surface dynamics, J. Chem. Phys. **131**, 024109 (2009).

[20] J. Prior, A. W. Chin, S. F. Huelga, and M. B. Plenio, Efficient simulation of strong system-environment interactions, Phys. Rev. Lett. **105**, 050404 (2010).

[21] N. Lambert, S. Ahmed, M. Cirio, and F. Nori, Modelling the ultra-strongly coupled spin-boson model with unphysical modes, Nat. Commun. **10**, 3721 (2019).

[22] Z. Tang, X. Ouyang, Z. Gong, H. Wang, and J. Wu, Extended hierarchy equation of motion for the spin-boson model, J. Chem. Phys. **143**, 224112 (2015).

[23] R. Hartmann, M. Werther, F. Grossmann, and W. T. Strunz, Exact open quantum system dynamics: Optimal frequency vs time representation of bath correlations, J. Chem. Phys. **150**, 234105 (2019).

[24] M. Xu, Y. Yan, Q. Shi, J. Ankerhold, and J. T. Stockburger, Taming quantum noise for efficient low temperature simulations of open quantum systems, Phys. Rev. Lett. **129**, 230601 (2022).

[25] R. P. Feynman and F. L. Vernon, The theory of a general quantum system interacting with a linear dissipative system, Ann. Phys. (Leipzig) **24**, 118 (1963).

[26] F. A. Pollock, C. Rodríguez-Rosario, T. Frauenheim, M. Paternostro, and K. Modi, Non-Markovian quantum processes: Complete framework and efficient characterization, Phys. Rev. A **97**, 012127 (2018).

[27] D. E. Makarov and N. Makri, Path integrals for dissipative systems by tensor multiplication. Condensed phase quantum dynamics for arbitrarily long time, Chem. Phys. Lett. **221**, 482 (1994).

[28] M. R. Jørgensen and F. A. Pollock, Exploiting the causal tensor network structure of quantum processes to efficiently simulate non-Markovian path integrals, Phys. Rev. Lett. **123**, 240602 (2019).

[29] F. Otterpohl, P. Nalbach, and M. Thorwart, Hidden phase of the spin-boson model, Phys. Rev. Lett. **129**, 120406 (2022).

[30] G. E. Fux, E. P. Butler, P. R. Eastham, B. W. Lovett, and J. Keeling, Efficient exploration of Hamiltonian parameter space for optimal control of non-Markovian open quantum systems, Phys. Rev. Lett. **126**, 200401 (2021).

[31] G. E. Fux, D. Kilda, B. W. Lovett, and J. Keeling, Tensor network simulation of chains of non-Markovian open quantum systems, Phys. Rev. Res. **5**, 033078 (2023).

[32] P. Fowler-Wright, B. W. Lovett, and J. Keeling, Efficient many-body non-Markovian dynamics of organic polaritons, Phys. Rev. Lett. **129**, 173001 (2022).

[33] D. Gribben, D. M. Rouse, J. Iles-Smith, A. Strathearn, H. Maguire, P. Kirton, A. Nazir, E. M. Gauger, and B. W. Lovett, Exact dynamics of nonadditive environments in non-Markovian open quantum systems, PRX Quantum **3**, 010321 (2022).

[34] F. Verstraete, J. J. García-Ripoll, and J. I. Cirac, Matrix product density operators: Simulation of finite-temperature and dissipative systems, Phys. Rev. Lett. **93**, 207204 (2004).

[35] M. Zwolak and G. Vidal, Mixed-state dynamics in one-dimensional quantum lattice systems: A time-dependent superoperator renormalization algorithm, Phys. Rev. Lett. **93**, 207205 (2004).

[36] G. Vidal, Classical simulation of infinite-size quantum lattice systems in one spatial dimension, Phys. Rev. Lett. **98**, 070201 (2007).

[37] We assume without loss of generality that $\mathrm{tr}\rho_{\mathrm{env}}(0)B(t) = 0$.

[38] V. Link, W. T. Strunz, and K. Luoma, Non-Markovian quantum dynamics in a squeezed reservoir, Entropy **24**, 352 (2022).

[39] N. Hatano and M. Suzuki, Finding exponential product formulas of higher orders, in *Quantum Annealing and Other Optimization Methods* (Springer, Berlin, 2005), pp. 37–68.

[40] N. Makri and D. E. Makarov, Tensor propagator for iterative quantum time evolution of reduced density matrices. I. Theory, J. Chem. Phys. **102**, 4600 (1995).

[41] N. Makri and D. E. Makarov, Tensor propagator for iterative quantum time evolution of reduced density matrices. II. Numerical methodology, J. Chem. Phys. **102**, 4611 (1995).

[42] M. Cygorek, M. Cosacchi, A. Vagov, V. M. Axt, B. W. Lovett, J. Keeling, and E. M. Gauger, Simulation of open quantum systems by automated compression of arbitrary environments, Nat. Phys. **18**, 662 (2022).

[43] See Supplemental Material at http://link.aps.org/supplemental/10.1103/PhysRevLett.132.200403 for mathematical and numerical details, which contains Ref. [45].

[44] X. Gao, J. Ren, A. Eisfeld, and Z. Shuai, Non-Markovian stochastic Schrödinger equation: Matrix-product-state approach to the hierarchy of pure states, Phys. Rev. A **105**, L030202 (2022).

[45] The TEMPO Collaboration, OQuPy (2023), https://github.com/tempoCollaboration/OQuPy.

[46] This is no restriction because the system evolution for N time steps only depends on $\alpha(t)$ for $t < N\Delta$. Thus, if the correlation function does not decay, we can add an artificial smooth cutoff to the bath correlation for times after $t = N\Delta$.

[47] M. Cygorek, J. Keeling, B. W. Lovett, and E. M. Gauger, Sublinear scaling in non-Markovian open quantum systems simulations, Phys. Rev. X **14**, 011010 (2024).

[48] R. Orús and G. Vidal, Infinite time-evolving block decimation algorithm beyond unitary evolution, Phys. Rev. B **78**, 155117 (2008).

[49] An open source implementation of the iTEBD based method is available at https://github.com/val-link/iTEBD-TEMPO.

[50] R. Hartmann and W. T. Strunz, Environmentally induced entanglement—anomalous behavior in the adiabatic regime, Quantum **4**, 347 (2020).

[51] F. Minganti, A. Biella, N. Bartolo, and C. Ciuti, Spectral theory of Liouvillians for dissipative phase transitions, Phys. Rev. A **98**, 042118 (2018).

[52] B. Debecker, J. Martin, and F. Damanet, Spectral theory of non-Markovian dissipative phase transitions, arXiv:2307.01119.

[53] R. Hartmann and W. T. Strunz, Accuracy assessment of perturbative master equations: Embracing nonpositivity, Phys. Rev. A **101**, 012103 (2020).

[54] C. H. Fleming and N. I. Cummings, Accuracy of perturbative master equations, Phys. Rev. E **83**, 031117 (2011).

[55] E. Crowder, L. Lampert, G. Manchanda, B. Shoffeitt, S. Gadamsetty, Y. Pei, S. Chaudhary, and D. Davidović, Invalidation of the Bloch-Redfield equation in the sub-Ohmic regime via a practical time-convolutionless fourth-order master equation, Phys. Rev. A **109**, 052205 (2024).

[56] R. Palacino and J. Keeling, Atom-only theories for U(1) symmetric cavity-QED models, Phys. Rev. Res. **3**, L032016 (2021).

[57] R. Bulla, N.-H. Tong, and M. Vojta, Numerical renormalization group for bosonic systems and application to the sub-Ohmic spin-boson model, Phys. Rev. Lett. **91**, 170601 (2003).

[58] M. Vojta, N.-H. Tong, and R. Bulla, Quantum phase transitions in the sub-Ohmic spin-boson model: Failure of the quantum-classical mapping, Phys. Rev. Lett. **94**, 070604 (2005).

[59] F. B. Anders, R. Bulla, and M. Vojta, Equilibrium and nonequilibrium dynamics of the sub-Ohmic spin-boson model, Phys. Rev. Lett. **98**, 210402 (2007).

[60] H. Wang and M. Thoss, From coherent motion to localization: II. Dynamics of the spin-boson model with sub-Ohmic spectral density at zero temperature, Chem. Phys. **370**, 78 (2010).

[61] P. Nalbach and M. Thorwart, Ultraslow quantum dynamics in a sub-Ohmic heat bath, Phys. Rev. B **81**, 054308 (2010).

[62] P. Nalbach and M. Thorwart, Crossover from coherent to incoherent quantum dynamics due to sub-Ohmic dephasing, Phys. Rev. B **87**, 014116 (2013).

[63] J. Ren, W. Li, T. Jiang, Y. Wang, and Z. Shuai, Time-dependent density matrix renormalization group method for quantum dynamics in complex systems, WIREs Comput. Mol. Sci. **12**, e1614 (2022).

[64] H. Wang and J. Shao, Quantum phase transition in the spin-boson model: A multilayer multiconfiguration time-dependent Hartree study, J. Phys. Chem. A **123**, 1882 (2019).

[65] V. Zauner-Stauber, L. Vanderstraeten, M. T. Fishman, F. Verstraete, and J. Haegeman, Variational optimization algorithms for uniform matrix product states, Phys. Rev. B **97**, 045145 (2018).

[66] L. Vanderstraeten, J. Haegeman, and F. Verstraete, Tangent-space methods for uniform matrix product states, SciPost Phys. Lect. Notes **7** (2019).

[67] B. Vanhecke, M. V. Damme, J. Haegeman, L. Vanderstraeten, and F. Verstraete, Tangent-space methods for truncating uniform MPS, SciPost Phys. Core **4**, 004 (2021).

[68] N. Ng, G. Park, A. J. Millis, G. K.-L. Chan, and D. R. Reichman, Real-time evolution of Anderson impurity models via tensor network influence functionals, Phys. Rev. B **107**, 125103 (2023).